

# A Novel Flame Chemiluminescence Measurement using a Digital Colour Camera

Jiansheng Yang, Zhen Ma and Yang Zhang

Department of Mechanical Engineering, the University of Sheffield  
Sheffield, South Yorkshire, UK

## 1 Introduction

Flame chemiluminescence measurement is a useful combustion diagnostics tool. Chemiluminescent emission occurs when excited molecules within a combustion reaction return to their ground state and emit photons at specific wavelengths [1]. For a premixed hydrocarbon flame, the visible greenish-blue colour is mostly attributed to the presence and the mixture of  $\text{CH}^*$  and  $\text{C}_2^*$  emissions [2]. Many studies have shown that the  $\text{CH}^*$  and  $\text{C}_2^*$  concentrations exhibit non-monotonic dependence on equivalence ratio ( $\Phi$ ) of a flame [3,4]. Besides, the  $\text{CH}^*/\text{C}_2^*$  chemiluminescence ratio has been shown have a linear response to  $\Phi$  [5]. Therefore, chemiluminescence measurement is considering as a relative way for  $\Phi$  measurement [6,7].

In the past, flame species were measured by sampling probes [8]. Flame spectral analysis can provide qualitative information of fuel/air ratio, but lacks of the temporal and spatial information. Some researchers employed monochrome camera connecting with different narrow wavelength filters to obtain local emission concentrations of different radicals, such as  $\text{CH}^*$  ( $430 \pm 5$  nm) and  $\text{C}_2^*$  ( $516 \pm 5$  nm) [9,10]. In this method, the  $\text{CH}^*$  and  $\text{C}_2^*$  concentrations need captured separately, which is not suitable for measuring a fast phenomenon, such as explosion. Recently, Huang proposed a model which employ image mean blue and green intensities to present the global concentration of  $\text{CH}^*$  and  $\text{C}_2^*$  respectively [11]. His method can detect  $\text{CH}^*$  and  $\text{C}_2^*$  concentrations at the same time by a simple colour camera. However, because of the sensor spectral sensitivity difference within different cameras, Migliorini could not repeat Huang's result by simply using Huang's model [12]. The aim of this work is to propose a more flexible model to detect  $\text{CH}^*$  and  $\text{C}_2^*$  concentrations by image colour.

## 2 Methodology

In the CFA (Colour Filter Array) scheme, a colour camera sensor has three primary channels  $R$ ,  $G$  and  $B$  (Red, Green and Blue respectively). The colour displaying at a pixel is the combination of the values on these three channels. Therefore, an apparent colour of the visible light striking on a pixel could be defined as  $C = [I_R, I_G, I_B]$ , where  $C$  indicates the presented colour by a pixel.  $I$  is the intensity of each channel. The intensity of each colour channel for a pixel is the sum of radiations from all the visible wavelengths (400 - 700 nm, for example). Thus, the intensities of three colour channels can be defined as

$$\begin{cases} I_R = \sum_{i=400}^{700} I_{R_i} \\ I_G = \sum_{i=400}^{700} I_{G_i} \\ I_B = \sum_{i=400}^{700} I_{B_i} \end{cases} \quad (1)$$

where  $i$  denotes the wavelength in nanometre. Similar to the long, middle and short wavelength cones in human eyes, the spectral sensitive range of the  $R$ ,  $G$  and  $B$  colour channels are different. Therefore, for a certain wavelength, the spectral sensitivities for three colour channels are different. As spectral sensitivity varies in three channels, in general, the normal sensitivity relationship among these three colour channels could be written as

$$\frac{I_R}{\alpha_{R_i}} = \frac{I_G}{\alpha_{G_i}} = \frac{I_B}{\alpha_{B_i}}, \quad (2)$$

where  $\alpha$  denotes the colour channel sensitivity at a certain wavelength.

For a premixed hydrocarbon flame, the flame chemiluminescences are mostly contributed to the presence and the mixture of  $\text{OH}^*$ ,  $\text{CH}^*$  and  $\text{C}_2^*$  radical emissions in the UV-VIS spectrum [2]. The modern digital colour camera can only capture light in VIS spectrum, while the  $\text{OH}^*$  emission is in UV spectrum. Due to the  $\text{OH}^*$  cannot be measured directly by normal cameras, only  $\text{CH}^*$  and  $\text{C}_2^*$  are measured in the proposed method. Various experiments have demonstrated that the  $\text{CH}^*$  and  $\text{C}_2^*(0,0)$  emissions are dominated at 430 nm and 516.5 nm wavelengths, respectively [2]. Therefore, in this method, we assume that the colour of a premixed hydrocarbon flame is only contributed to the photons emitted at 430 and 516 nm wavelengths. Based on this assumption, Eq. (1) could be simplified as:

$$\begin{cases} I_R = I_{R_{430}} + I_{R_{516}} \\ I_G = I_{G_{430}} + I_{G_{516}} \\ I_B = I_{B_{430}} + I_{B_{516}} \end{cases} \quad (3)$$

Due to the variance of spectral sensitivity among  $R$ ,  $G$  and  $B$ , the  $R$  channel in most camera sensors is not sensitive to both 430 and 516 nm. Thus, here we only utilise two channels,  $B$  and  $G$  in the proposed method. Based on Eq. (2), the intensities relationships between  $G$  and  $B$  channels at 430 and 516 nm wavelengths as shown below:

$$I_{B_{430}} = \lambda_1 I_{G_{430}}, \quad (4)$$

$$I_{B_{516}} = \lambda_2 I_{G_{516}}, \quad (5)$$

where  $\lambda_1$  indicates  $\frac{\alpha_{B_{430}}}{\alpha_{G_{430}}}$ ,  $\lambda_2$  indicates  $\frac{\alpha_{B_{516}}}{\alpha_{G_{516}}}$ .

For cameras whose  $G$  channel is sensitive to 430 nm, thus both  $G$  and  $B$  intensities are the mixture of emissions at 430 and 516 nm wavelengths. So, we have

$$\begin{cases} I_G = I_{G_{430}} + I_{G_{516}} \\ I_B = I_{B_{430}} + I_{B_{516}} = \lambda_1 I_{G_{430}} + \lambda_2 I_{G_{516}} \end{cases} \quad (6)$$

Then, we obtain the  $\text{CH}^*$  and  $\text{C}_2^*$  chemiluminescence expression:

$$\begin{cases} I_{\text{CH}^*} = I_{B_{430}} = \frac{\lambda_1 \lambda_2 I_G - \lambda_1 I_B}{\lambda_1 - \lambda_2} \\ I_{\text{C}_2^*} = I_{B_{516}} = \frac{\lambda_2 I_B - \lambda_1 \lambda_2 I_G}{\lambda_2 - \lambda_1} \end{cases} \quad (7)$$

For the cameras that  $G$  channel is non-sensitive to 430 nm wavelengths, hence the  $G$  intensity is the only attribute to radiation at 516 nm wavelength and  $B$  intensity value is the mixing intensities attributing to both radiations at 430 and 516 nm wavelengths. So Eq. (3) can be rewritten as

$$\begin{cases} I_G = I_{G_{516}} \\ I_B = I_{B_{430}} + I_{B_{516}} = I_{B_{430}} + \lambda_2 I_{G_{516}} \end{cases} \quad (8)$$

Finally we obtained the  $\text{CH}^*$  and  $\text{C}_2^*$  chemiluminescence expression:

$$\begin{cases} I_{CH^*} = I_{B_{430}} = I_B - \lambda_2 I_G \\ I_{C_2^*} = I_{B_{516}} = \lambda_2 I_G \end{cases} \quad (9)$$

### 3 Experimental setup and process

The experiments are performed on a free-burning atmospheric burner with the inner nozzle diameter of 10 mm. The premixed  $C_3H_8$  flames are measured at equivalence ratios from 0.93 to 1.53 (12 cases with constant fuel flow rate of 0.105 L/min by varying the premixing air flow rates from 1.7 to 2.8 L/min, with 0.1 L/min interval to obtain the desired equivalence ratio states). A Photron SA-4 high-speed colour camera is employed for testing the proposed method. In each case, 2000 image frames were captured at settings of 125 fps with 1/125s shutter speed at steady burning state (5 minutes interval between data acquisition).

The employed camera sensor sensitivity calibration setup needs a standard light source and a monochromator to allow ray passing through onto camera sensor at a specific wavelength. The standard light source used here was an approximated black-body radiator in the form of a 150 W tungsten lamp powered by a 12 V battery. The Newport Manual Mini Monochromator (Model 78022) is used to produce monotonic spectral variations for camera photograph. Using this setup, the  $R$ ,  $G$  and  $B$  colour channels spectral responses of the employed camera sensor are calibrated from 400 to 700 nm with a 10 nm interval. The measured tungsten radiance is fixed at the temperature of 2200 °C. The captured image data are saved as 16-bit TIFF format. For each image, the average intensity of each colour channel is recorded. The results are normalised by dividing the maximum pixel value of  $2^{16}$ , as shown in Figure 1.

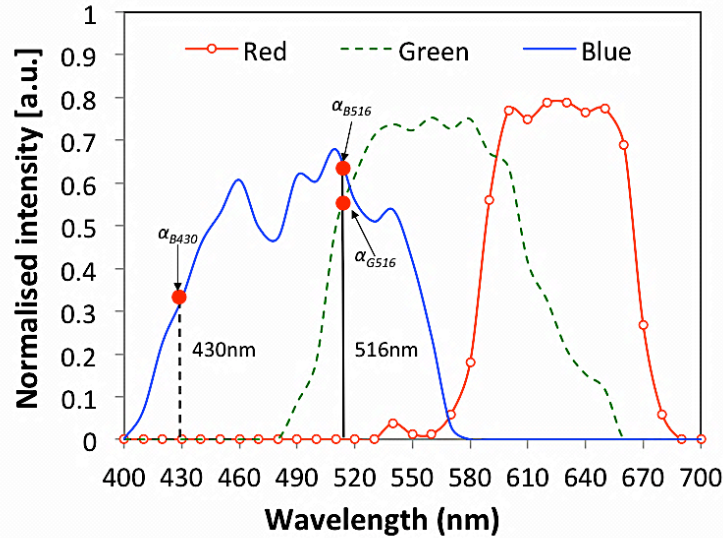


Figure 1:  $R$ ,  $G$  and  $B$  channel spectral sensitivities of employed camera.

According to the above figure, the  $CH^*$  emission at 430 nm is only sensitive by  $B$  channel, whereas the  $C_2^*$  emission at 516 nm can be sensed by both  $G$  and  $B$  channel. Channel  $R$  does not cover neither 430 nor 516 nm. From the figure we can see that the  $G$  channel of the employed camera is not sensitive to 430 nm wavelength, therefore the further calibration will use Eq. (9). According to Figure 1, the normalised radiation transmission ratio  $\alpha$  of  $B$  and  $G$  channels at 516 nm are about 0.62 and 0.56 respectively. Therefore, the approximation of  $\lambda_2$  is equal to 1.1. The  $CH^*$  and  $C_2^*$  chemiluminescence expressions based on the employed camera are

$$\begin{cases} I_{CH^*} \approx I_B - 1.1I_G \\ I_{C_2^*} \approx 1.1I_G \end{cases} \quad (10)$$

It is necessary to be emphasized here that the Eq. 10 is only satisfied for the camera employed in this work. Since the spectral responses of  $R$ ,  $G$  and  $B$  channels are different in different cameras, the sensitivity ratio  $\alpha$  is also a camera specific parameter. For different cameras, this parameter can be obtained through camera sensor calibration. This may also explain the cause of Migliorini failing to reproduce Huang's results even using Huang's method as mentioned before [12].

The image processing is conducted on Matlab. The original digital image colour is in RGB colour model. In order to select the premixed flame easily, the image is converted from RGB to HSV model. According to the previous investigation by Huang, the digital colour representative of hydrocarbon premixed flame chemiluminescence is in the range of  $120^\circ$  -  $240^\circ$  within hue [14]. Therefore, the colour values within this region are selected. Only the radiation colour intensity of the conic flame zone was extracted for the computation, neglecting the green/blue emission of the surrounding  $CO-O^*$  sheath. The processed image data at different equivalence ratios are plotted in Figure 2. In order to visualise flame clearly, these processed image are enhanced 10 times in their primary intensity values in  $R$ ,  $G$  and  $B$  channels respectively.

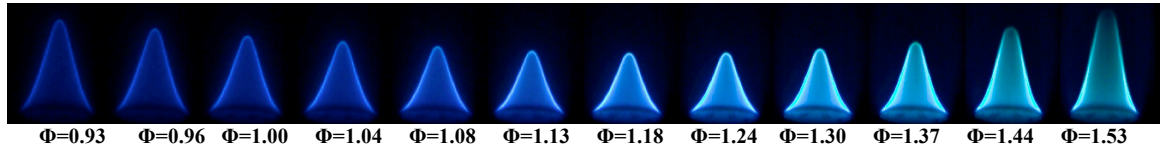


Figure 2: Processed  $C_3H_8$  premixed flame images at equivalence ratio  $\Phi$  ranges from 0.93 to 1.53, the  $R$ ,  $G$  and  $B$  intensities of each image are enhanced 10 times.

## 4 Results and analysis

As shown in Figure 2, from left to right, as  $\Phi$  increase, the colour of flame turns from pure blue to green-blue. It is because more  $C_2^*$  would occur in high equivalence ratio condition. The corresponding local  $CH^*/C_2^*$  chemiluminescence emission ratio map that is calculated using Eq. 10 are shown in Figure 3. Almost all the regions of one local  $I_{CH}/I_{C_2}$  ratio map is in the same colour or changed slightly, it means that the colour-calculated local  $I_{CH}/I_{C_2}$  ratio is constant or slightly different. Since the fuel and air are well premixed, it also indicates that the proposed colour-calculated chemiluminescence method has the potential to measure fuel/air ratio accurately.

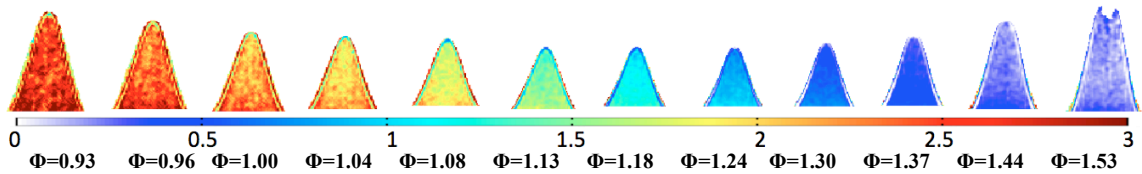


Figure 3: Colour-calculated  $I_{CH}/I_{C_2}$  ratio maps at equivalence ratio ranges from 0.93 to 1.53 for Figure 2.

A quantitative parametric investigation was further analysed to assess the variation between the  $\Phi$  and the corresponding colour signal distributions. The typical histogram of the computed  $I_{CH}/I_{C_2}$  ratio follows a normal distribution profile is shown in Figure 4a. These distributions are then fitted by the Gaussian distribution to calculate the acquired mean and variance ( $\mu_e$  and  $\sigma^2$  respectively).

The observed discrete variation of the  $\mu_e$  values suggests that a curve fitting algorithm can be applied to compute the corresponding  $\Phi$  state based on the statistical  $\mu_e$  of the  $I_{CH}/I_{C_2}$  ratio distribution. It is however evident from Fig 4a, that the broadness of the distribution means that addition step needs to be taken to evaluate the accuracy of  $\mu_e$  and its range of deviation. To facilitate this, 500 frames from each dataset (comprising of 1500 images per dataset) were used to as training-data to predict the

average  $\mu_e$  as well as its upper and lower limits at a  $CI$  (confidence interval) of 99%. From the remaining 1000 frames, the  $\mu_e$  from five data groups (each ensembles 100 random image frames) were calculated and compared with the training-data.

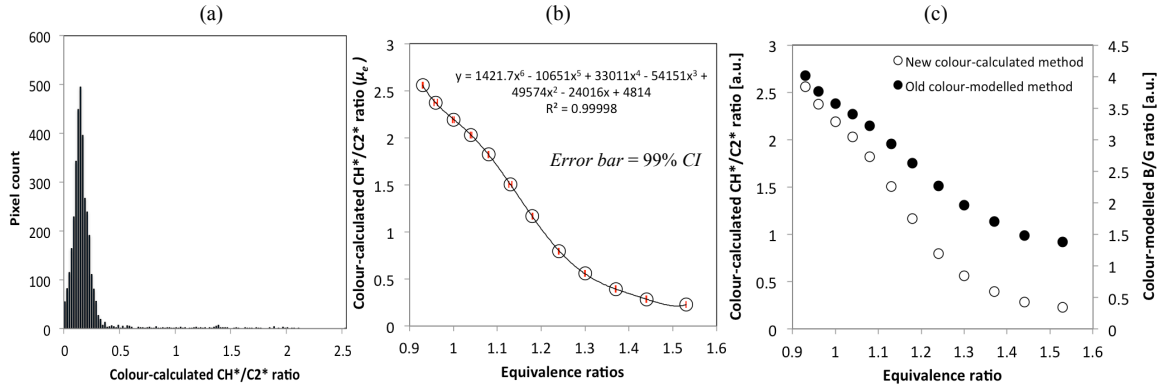


Figure 4: (a) Typical single frame  $\mu_e$  histogram at  $\Phi = 1.44$ ; (b) Calculated  $\mu_e$  values at different  $\Phi$  along with error bar denoting the 99%  $CI$  range; (c) Comparison between Huang's colour-dived B/G ratio (Y-left axis) and proposed.

As it can be seen in Fig. 4b, the computed Gaussian distribution of the  $\mu_e$  population illustrates discrete  $\mu_e$  peaks from  $\Phi = 0.93$  to 1.53. The trend of the characteristic  $\mu_e$  corresponding to the different  $\mu_e$  varies almost linearly from  $\Phi = 0.93$  to 1.53. As it can be seen even at 99%  $CI$ , the variation of the computed  $\mu_e$  is small; the upper and lower limits are typically less than 1% from each characteristic  $\mu_e$  at different  $\Phi$ . The maximum  $\mu_e$  deviation is no greater than 2% from its characteristic  $\mu_e$  predicted from the training-data; meaning a maximum of 1% deviation from the 99%  $CI$  range. Therefore the actual fluctuation of the average  $\mu_e$  value is small.

The same data was also processed by Huang's colour-modelled chemiluminescence measurement method. In his colour-modelled method, the  $CH^*$  and  $C_2^*$  concentration results are simply indicated by image average blue and green intensities, respectively. The comparison of the two methods is shown in Figure 4c. The colour-modelled method results indicate in the black ball with Y-right axis while the proposed colour-calculated method results are shown by the white ball with Y-left axis. The main trends of the both results are similar that the ratio becomes smaller during equivalence ratio increases from 0.93 to 1.53. However, the ratio decreases faster in the proposed colour-calculated method, which makes the difference between results from this two methods become larger when equivalence ratio increases.

## 5 Conclusion

A novel flame  $CH^*$  and  $C_2^*$  chemiluminescence measurement using a digital colour camera is proposed. This method is based on assumption of the premixed flame chemiluminescence only attributed to  $CH^*$  emission at 430 nm and  $C_2^*$  emission at 516 nm. A camera sensor calibration is needed to detect different specific parameters for correcting the spectral sensitivity difference in different cameras. The  $CH^*$  and  $C_2^*$  concentration can be present by

$$\begin{cases} I_{CH^*} = I_{B_{430}} = \frac{\lambda_1 \lambda_2 I_G - \lambda_1 I_B}{\lambda_1 - \lambda_2} \\ I_{C_2^*} = I_{B_{516}} = \frac{\lambda_2 I_B - \lambda_1 \lambda_2 I_G}{\lambda_2 - \lambda_1} \end{cases} \text{ or } \begin{cases} I_{CH^*} = I_{B_{430}} = I_B - \lambda_2 I_G \\ I_{C_2^*} = I_{B_{516}} = \lambda_2 I_G \end{cases}, \text{ depending on the spectral sensitivity}$$

of  $G$  channel. This method has been estimated by measuring  $C_3H_8$  premixed flame from  $\Phi = 0.93$  to

1.53. The detected maximum global  $I_{CH}/I_{C2}$  deviation is no greater than 2% from its characteristic global  $I_{CH}/I_{C2}$  predicted from the training-data; meaning a maximum of 1% deviation from the 99% CI range. Compared with conventional colour-modelled chemiluminescence measurement, the trends of the results obtained from both methods are similar in the beginning and their difference increases in higher  $\Phi$  conditions. This model can measure  $CH^*$  and  $C_2^*$  concentrations, and it shows a great potential in measuring local  $\Phi$  with a satisfied accuracy.

## References

- [1] French AP, Taylor EF. (1998). An Introduction to Quantum Physics. Cheltenham: Stanley Thornes.
- [2] Gaydon AG, Wolfhard HW. (1979). Flames-their structure, radiation and temperature. London: Chapman and Hall.
- [3] Schefer RW. (1997). Flame sheet imaging using CH chemiluminescence. Combust. Sci. Technol. 126: 255-270.
- [4] Kojima J, Ikeda Y, Nakajima T. (2000). Spatially resolved measurement of  $OH^*$ ,  $CH^*$  and  $C_2^*$  chemiluminescence in the reaction zone of laminar methane/air premixed flames. Proc. Comb. Ins. 28 : 1757-1764.
- [5] Haber LC. (2000). An investigation into the origin, measurement and application of chemiluminescent light emissions from premixed flames. Master Thesis, Mechanical Engineering Faculty of the Virginia Polytechnic Institute and State University.
- [6] Chou T, Patterson DJ. (1995). In-cylinder measurement of mixture maldistribution in a L-head engine. Combust. Flame. 101: 45-57.
- [7] Higgins B. et al. (2001). An experimental study on the effect of pressure and strain rate on CH chemiluminescence of premixed fuel-lean methane/air flames. Fuel. 80: 1583-1591.
- [8] Taylor AMKP. (1993). Instrumentation for flows with combustion. San Diego Academic Press.
- [9] Nori V, Seitzman J. (2008). Evaluation of chemiluminescence as a combustion diagnostic under varying operating conditions. AIAA paper, 953.
- [10] Worth NA, Dawson JR. (2013). Tomographic reconstruction of  $OH^*$  chemiluminescence in two interacting turbulent flames. Measurement Science and Technology, 24(2), 024013.
- [11] Huang HW, Zhang Y. (2011). Digital colour image processing based measurement of premixed  $CH_4$ +air and  $C_2H_4$ +air flame chemiluminescence. Fuel. 19: 48-53.
- [12] Migliorini FSM. et al. (2014). Analysis of chemiluminescence measurements by grey-scale ICCD and colour digital cameras. Measurement Science and Technology. 25, 055202.
- [13] Huang HW, Zhang Y. (2008). Flame colour characterization in the visible and infrared spectrum using a digital camera and image processing. Measurement Science and Technology. 19, 085406.